Proceedings of the
International Conference on Mechanical Engineering 2011
(ICME2011) 18- 20 December 2011, Dhaka, Bangladesh

ICME11-FL-037

STUDY ON CHARACTERISTICS OF REAL GAS FLOW THROUGH A CRITICAL NOZZLE

Mamun Mohammad[1], Junji Nagao[2], Shigeru Matsuo[3], Toshiaki Setoguchi[4] and Heuy Dong Kim[5]

[1] Dept. of Mechanical Engineering, BUET, Dhaka, Bangladesh.
[2] Graduate School of Science and Engineering, Saga University, Saga, Japan.
[3] Dept. of Mechanical Engineering, Saga University, Saga , Japan.
[4] Institute of Ocean Energy, Saga University, Saga , Japan.
[5] School of Mechanical Engineering, Andong National University, Andong Korea.

ABSTRACT

A critical nozzle is used to measure the mass flow rate of gas. It is well known that the coefficient of discharge of the flow in a critical nozzle is a single function of the Reynolds number. The purpose of the present study are to investigate the real gas effect on discharge coefficient and thermodynamics properties through a critical nozzle by using H_2, N_2, CH_4 and CO_2, with the help of a CFD method and to clarify the relationship between mass flow rate of real gas flows at the nozzle throat and Reynolds number numerically Redlich-Kwong equation of state is employed to consider the force and volume effects of inter-molecules of these gases, and conservative equation of vibration energy is applied to investigate the effect of relaxation phenomena involving molecular vibration. It is incorporated into the axisymmetric, compressible Navier–Stokes equations. As a result, for working gases of H_2, N_2, CH_4 and CO_2, coefficient of discharge obtained by taking into account real gas effect decreased with an increase of Reynolds number. In high stagnation pressure, thermodynamic properties of real gas, such as the ratio of specific heats and compressibility factor changed compared with those of ideal gas. Vibration energy of CO_2 affected strongly the discharge coefficient and the ratio of specific heats compared with those of H_2, N_2 and CH_4. In high stagnation pressure, non-dimensional mass flow rate decreased with an increase of Reynolds number.

Keywords: Compressible Flow, Critical Nozzle, Real Gas Effects, Discharge Coefficient, Simulation.

1. INTRODUCTION

The minimum pressure ratio for the flow to choke is called the critical pressure ratio. Once choked, the flow is no longer dependent on the pressure change in the downstream flow field. In this case, the mass flow is determined only by the stagnation conditions upstream of the flow passage. The critical nozzle is defined as a device to measure the mass flow with only the nozzle supply conditions, making use of the flow-choking phenomenon at the nozzle throat.

In previous researches, much attention has been paid to the prediction of mass flow through a flow passage, since it was of practical importance in a variety of industrial and engineering fields. The mass flowrate and critical pressure ratio are associated with the working gas consumption and the establishment of safe operation conditions of the critical nozzle. According to previous researches [1-3], the mass flowrate and critical pressure ratio are strong functions of the Reynolds number.

Of many kinds of working gases employed in industrial field, it is being recognized that hydrogen gas is one of the most promising gases as a future alternative energy source. In such an application, precise measurement of flowrate is of practical importance for mileage and power output of the vehicle. A large number of works [4–7] has been made to investigate the thermo-physical properties of hydrogen gas, which are specified by some different kinds of the equations of state, the critical pressure, the compressibility factor of hydrogen gas and so on. However, only a few researches have been made to date on the mass flowrate of the high-pressure hydrogen gas through a critical nozzle, due to difficulties of treatment.

Recently, Nakao [8] has conducted the flowrate measurement of hydrogen gas using a critical nozzle, and has found that the discharge coefficient of hydrogen gas exceeds unity in a specific Reynolds number regime. He has vaguely inferred that this unreasonable value of the discharge coefficient would be due to real gas effects or any other measurement errors. No detailed explanation has been made for this abnormal discharge coefficient of high-pressure hydrogen gas.

The objectives in the present study are to investigate the real gas effect on discharge coefficient and

thermodynamics properties through a critical nozzle by using working gases of H_2, N_2, CH_4 and CO_2, with the help of a CFD method and to clarify the relationship between mass flow rate of real gas flows at the nozzle throat and Reynolds number numerically. Redlich - Kwong equation of state [9] is employed to consider the force and volume effects of inter-molecules of these gases, and conservative equation of vibration energy is applied to investigate the effect of relaxation phenomena involving molecular vibration. It is incorporated into the axisymmetric, compressible Navier–Stokes equations.

2. CFD ANALYSIS

2.1 Governing Equations

The governing equations, i.e., the unsteady compressible Navier-Stokes equations written in an axisymmetric coordinate system (x,y) are as follows :

$$\frac{\partial \boldsymbol{U}}{\partial t}+\frac{\partial \boldsymbol{E}}{\partial x}+\frac{\partial \boldsymbol{F}}{\partial y}=\frac{1}{Re}\left(\frac{\partial \boldsymbol{R}}{\partial x}+\frac{\partial \boldsymbol{S}}{\partial y}\right)+\frac{1}{y}\boldsymbol{H}_1+\boldsymbol{H}_2 \tag{1}$$

where

$$\boldsymbol{U}=\begin{bmatrix}\rho\\ \rho u\\ \rho v\\ E_t\\ \rho k\\ \rho\varepsilon\end{bmatrix},\ \boldsymbol{E}=\begin{bmatrix}\rho u\\ \rho u^2+p\\ \rho uv\\ u(E_t+p)\\ \rho ku\\ \rho\varepsilon u\end{bmatrix},\ \boldsymbol{F}=\begin{bmatrix}\rho v\\ \rho uv\\ \rho v^2+p\\ v(E_t+p)\\ \rho kv\\ \rho\varepsilon v\end{bmatrix},$$

$$\boldsymbol{R}=\begin{bmatrix}0\\ \tau_{xx}\\ \tau_{xy}\\ \alpha\\ \left(\mu+\frac{\mu_t}{\sigma_k}\right)\frac{\partial k}{\partial x}\\ \left(\mu+\frac{\mu_t}{\sigma_\varepsilon}\right)\frac{\partial \varepsilon}{\partial x}\end{bmatrix},\ \boldsymbol{S}=\begin{bmatrix}0\\ \tau_{xy}\\ \tau_{yy}\\ \beta\\ \left(\mu+\frac{\mu_t}{\sigma_k}\right)\frac{\partial k}{\partial y}\\ \left(\mu+\frac{\mu_t}{\sigma_\varepsilon}\right)\frac{\partial \varepsilon}{\partial y}\end{bmatrix},$$

$$\boldsymbol{H}_1=\begin{bmatrix}-\rho v\\ \tau_{xy}-\rho uv\\ \alpha-\rho v^2\\ \beta-(E_t+p)v\\ 0\\ 0\end{bmatrix},\ \boldsymbol{H}_2=\begin{bmatrix}0\\ 0\\ 0\\ 0\\ P_k-\rho\varepsilon\\ C_{1\varepsilon}\frac{\varepsilon}{k}P_k-C_{2\varepsilon}\rho\frac{\varepsilon^2}{k}\end{bmatrix} \tag{2}$$

$$E_t=\rho c_{\mathrm{v}}T+\frac{1}{2}\rho\left(u^2+v^2\right) \tag{3}$$

$$p=(\gamma-1)\left[E_t-\frac{1}{2}\rho\left(u^2+v^2\right)\right] \tag{4}$$

$$\alpha=u\tau_{xx}+v\tau_{yx}+\kappa\frac{\partial T}{\partial x},\ \beta=u\tau_{xy}+v\tau_{yy}+\kappa\frac{\partial T}{\partial y} \tag{5}$$

$$\mu_t=\rho C_\mu\frac{k^2}{\varepsilon} \tag{6}$$

$$P_k=2\mu_t\left[\left(\frac{\partial u}{\partial x}\right)^2+\frac{1}{2}\left(\frac{\partial v}{\partial x}+\frac{\partial u}{\partial y}\right)+\left(\frac{\partial v}{\partial y}\right)^2\right] \tag{7}$$

$$C_{1\varepsilon}=1.44,\ C_{2\varepsilon}=1.92,\ C_\mu=0.09,\ \sigma_k=1.0,\ \sigma_\varepsilon=1.3 \tag{8}$$

For working gases of H_2, N_2, CH_4 and CO_2, Redlich - Kwong equation was used to obtain the compressibility factor as follows [9]:

$$p=\frac{RT}{v-\tilde{b}}-\frac{a(T)}{v(v+b_0)} \tag{9}$$

where

$$a(T)=a_0\left(\frac{T_c}{T}\right) \tag{10}$$

$$\tilde{b}=b_0-c_0 \tag{11}$$

$$a_0=0.42747\frac{RT_c}{p_c} \tag{12}$$

$$b_0=0.08664\frac{RT_c}{p_c} \tag{13}$$

$$c_0=\frac{RT_c}{p_c+\frac{a_0}{v_c(v_c+b_0)}}+b_0-v_c \tag{14}$$

p_c, T_c and v_c are critical pressure, critical temperature, and critical specific volume, respectively. In Eq.(2), $\boldsymbol{U}$ is the conservative vector, $\boldsymbol{E}$ and $\boldsymbol{F}$ are inviscid flux vector and $\boldsymbol{R}$ and $\boldsymbol{S}$ are viscous flux vectors. $\boldsymbol{H}_1$ and $\boldsymbol{H}_2$ are the source terms corresponding to axisymmetry and turbulence, respectively. τ_{xx}, τ_{xy}, τ_{yx} and τ_{yy} are components of viscous shear stress.

In case with considering of the effect of vibration energy, following equation [10] are used in governing equation (Eq.(1));

$$\frac{\partial}{\partial t}(\rho\varepsilon_{\mathrm{v}})+\frac{\partial}{\partial x}(\rho u\varepsilon_{\mathrm{v}})+\frac{\partial}{\partial y}(\rho v\varepsilon_{\mathrm{v}})=-\frac{1}{r}\rho v\varepsilon_{\mathrm{v}}+\rho\dot{\varepsilon}_{\mathrm{v}} \tag{15}$$

where

$$\dot{\varepsilon}_{\mathrm{v}}=\frac{\varepsilon_{\mathrm{v}0}-\varepsilon_{\mathrm{v}}}{\tau_{\mathrm{v}}} \tag{16}$$

$$\varepsilon_{\mathrm{v}0}=\sum_{\mathrm{i}=1}^{\mathrm{K}}\frac{\theta_{\mathrm{i}}/T}{\exp(\theta_{\mathrm{i}}/T)-1}\frac{p}{\rho} \tag{17}$$

$$\tau_{\mathrm{v}}=C_1\frac{\exp(C_2/T)^{1/3}}{p} \tag{18}$$

θ_{i} and τ_{v} are characteristic temperature for vibration and relaxation time, respectively.

The governing equation systems that are

non-dimensionalized with reference values at the atmospheric condition are mapped from the physical plane into a computational plane of a general transform. To close the governing equations, standard k-ε model [11] is employed in computations. A third-order TVD (Total Variation Diminishing) finite difference scheme with MUSCL [12] is used to discretize the spatial derivatives, and a second order-central difference scheme for the viscous terms, and a second-order fractional step is employed for time integration.

2.2 Computational Conditions

Figure 1 shows an ISO-type toroidal throat sonic Venturi nozzle [13] used in the present study. The radius of curvature at the throat of the nozzle is twice the throat diameter ϕD (= 0.5935 mm). The nozzle has a diffuser with a half-angle θ = 3° and a length of three times the throat diameter. A sudden enlargement section that is 30D long and 30D high is connected to the exit of the diffuser. The nozzle inlet is located at 100D upstream of the nozzle throat.

The total pressure p_0 and back pressure p_b are given at the inlet and outlet of the critical nozzle, respectively. Total temperature of stagnation point is 298 K. The back pressure p_b is kept constant at 0.5p_0. The inlet total pressure p_0 is varied to change the Reynolds number.

Table 1 shows the ranges of Reynolds number in cases with vibration and no vibration.

3. RESULTS AND DISCUSSIONS

Figures 2(a), (b), (c) and (d) show relationships between Reynolds number and discharge coefficient for H_2, N_2, CH_4 and CO_2, respectively. For H_2 and N_2, present computations are good agreement with experimental results [14] in low Reynolds number. For an ideal gas assumption, the present computational results predict the coefficient of the discharge, which increases with the Reynolds number and then approaches a certain constant value [15]. However, the present computation taking into account the real gas effect is qualitatively similar to results obtained by Johnson [16] and Nakao [2]. For H_2, N_2 and CH_4, the coefficient of discharge of real gas with vibration is almost the same result compared with that of real gas without vibration. However, the coefficient of discharge of real gas with vibration for CO_2 is large compared with that of real gas without vibration. Unfortunately, a clear and persuasive reasoning for this is, at present, not known. Such a trend in the discharge coefficient can give rise to a significant error in the mass flow at high-pressure conditions. More studies are needed to elucidate this ambiguous problem.

Figures 3(a), (b), (c) and (d) show the mass fluxes at nozzle throat in high Reynolds number for H_2 (Re_{th} = 1,153,961), N_2 (Re_{th} = 107,629), CH_4 (Re_{th} = 100,000), CO_2 (Re_{th} = 90,000), respectively. As seen from these figure, a little difference between ideal and real gases is mainly recognized in the region outside the boundary layer and the mass flux of real gas becomes slightly small. It is considered that a decrease of C_d with an increase of Reynolds number in case of real gas in Fig.2 is due to the decrease of mass flux. For H_2, N_2 and CH_4, the mass fluxes with vibration are almost the same result in comparison with that of without vibration. However, the mass flux with vibration for CO_2 is large compared with that of no vibration.

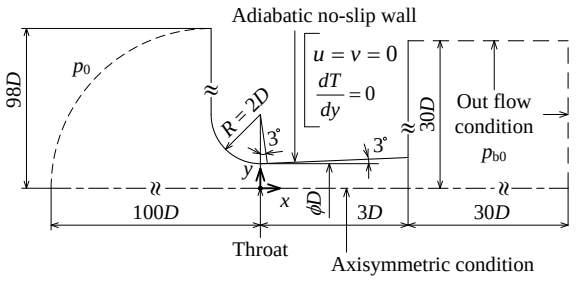

Fig 1. Boundary condition

Table 1: Reynolds number for without vibration and with vibration

	Without vibration	With vibration
Hydrogen	2,155-1,153,961	2,155 / 200,509 / 1,153,961
Nitrogen	5,400-203,727	5,400 / 10,800 / 107,629
Methane	5,100-200,000	5,100 / 19,500 /100,000
Carbon dioxide	5,810-201,000	5,810 / 22,000 / 90,000

Figures 4(a), (b), (c) and (d) show the relationships between Reynolds number and ratio of specific heats at nozzle throat. Note that ratios of specific heats of ideal gas for H_2, N_2, CH_4 and CO_2 are constant at 1.41 (H_2), 1.40 (N_2), 1.30 (CH_4) and 1.29 (CO_2), respectively. For H_2 and N_2, distributions of ratio of specific heats for both the real and ideal gases are nearly the same in low Reynolds number. However, ratios of specific heats of real gas for CH_4 and CO_2 are large compared with that of ideal gas in low Reynolds number. Further, ratios of specific heats decrease with an increase of Reynolds number in high Reynolds number. The difference between vibration and no vibration for CO_2 is largest compared with H_2, N_2 and CH_4. This variation in the ratio of specific heats has a significant influence on the mass flow.

Figure 5 show the relationships between Reynolds number and compressibility factor at nozzle throat. If the gas is assumed to be an ideal gas, the compressibility factor is 1.0 regardless of Reynolds number. As seen from this figure, compressibility factor for real gas is 1.0 in low Reynolds number. However, in high Reynolds number, compressibility factor for N_2, CH_4 and CO_2 decrease with an increase of Reynolds number. For H_2, compressibility factor increases with Reynolds number.

Figure 6 shows relationships between mass flowrate of real gas at nozzle throat and pressure ratio for H_2 in the range from Re_{th} = 613 to 1,153,961. Solid line indicates the mass flow rate obtained by one-dimensional theory. As seen from this figure, in the range from Re_{th} = 613 to 200,509, the mass flow rate increases with an increase of Reynolds number for each pressure ratio. However, in the range from Re_{th}=384,650 to 1,153,961, the mass flow rate decreases with an increase of Reynolds number for each pressure ratio.

4. CONCLUSIONS

A computational study has been made to investigate the flow features of air through the critical nozzle. In order to simulate the real gas effects which appear at high-pressure conditions, Redlich-Kwong equation of state has been employed for H_2, N_2, CH_4 and CO_2, and incorporated into the axisymmetric, compressible Navier–Stokes equations. The results obtained are as

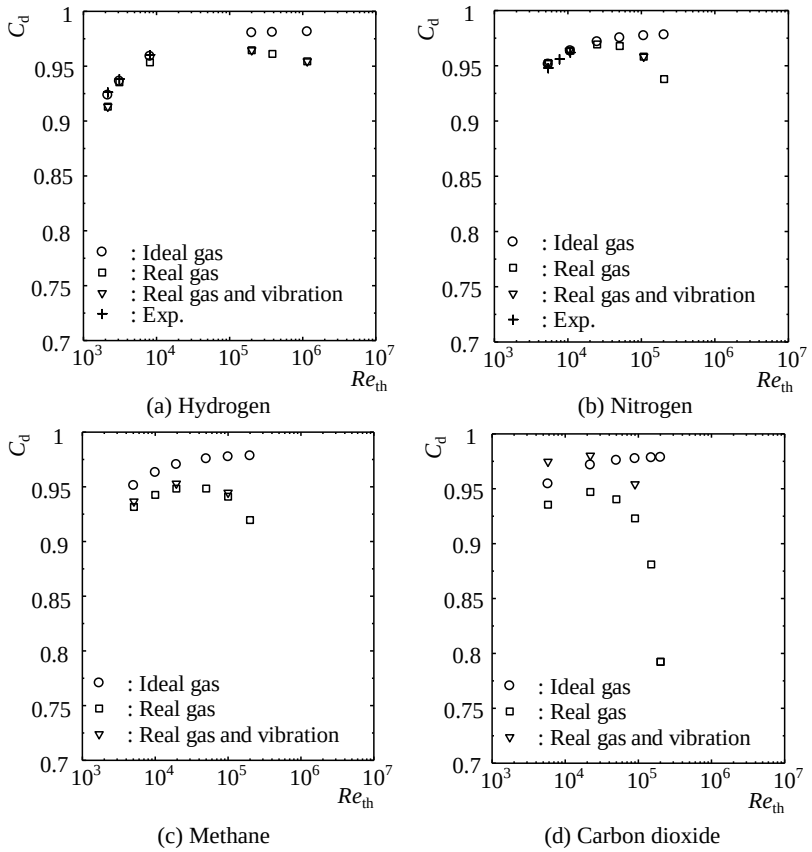

Fig 2. Relationships between Reynolds number and discharge coefficient

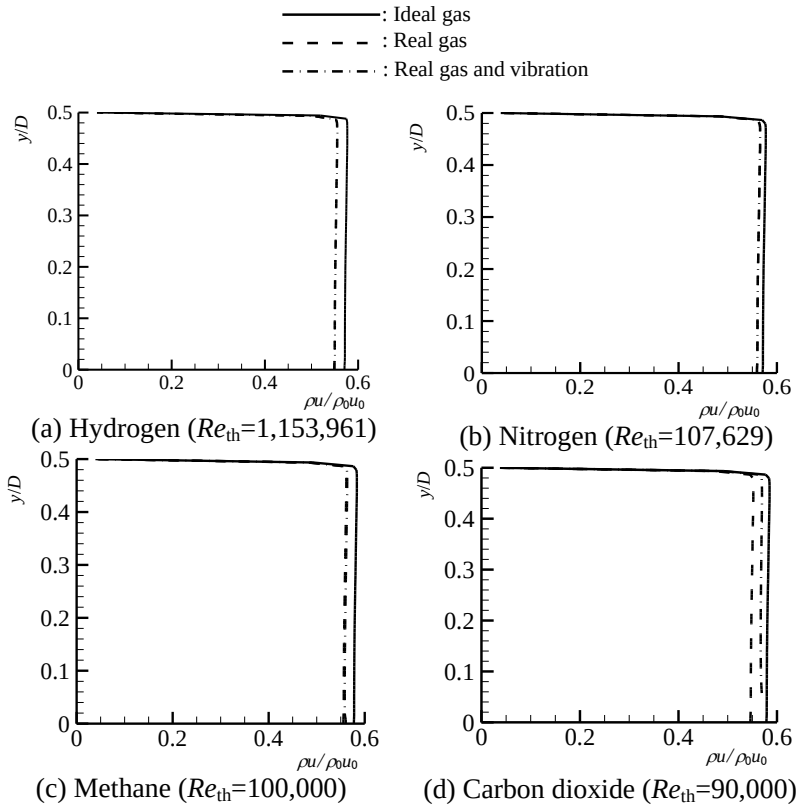

Fig 3. Mass fluxes at nozzle throat

follows : The coefficient of discharge of real gas at nozzle throat decreased with an increase of Reynolds number. Mass fluxes of real gas became small compared with ideal gas with an increase of Reynolds number. In high Reynolds number, the thermodynamics properties of real gas, such as the compressibility factor and the ratio of specific heats changed compared with ideal gas. Vibration energy of CO_2 affected strongly the discharge coefficient and the ratio of specific heats compared with those of H_2, N_2 and CH_4. In high Reynolds number, non-dimensional mass flow rate decreased with an increase of Reynolds number.

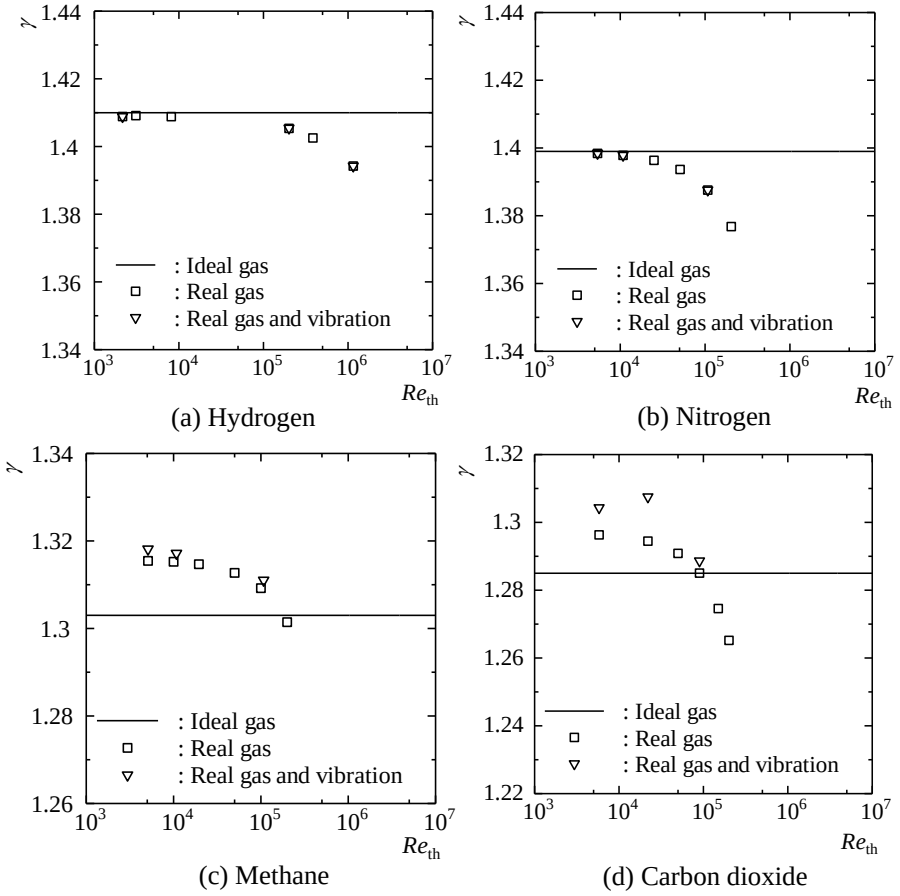

Fig 4. Relationships between Reynolds number and ratio of specific heats at nozzle throat

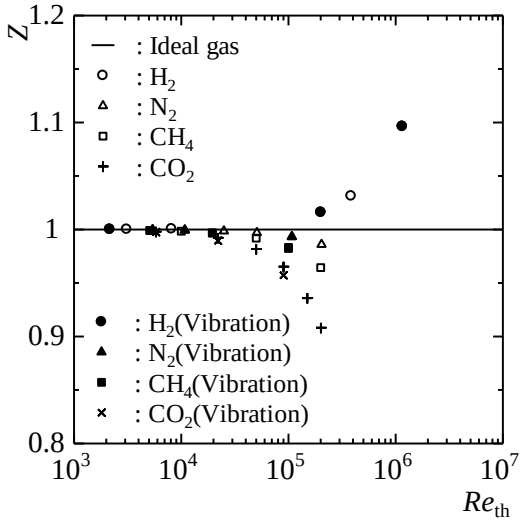

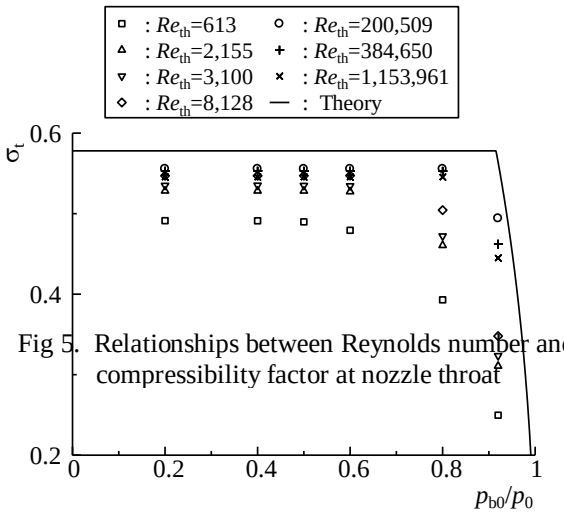

Fig 5. Relationships between Reynolds number and compressibility factor at nozzle throat

5. REFERENCES

1. Tang, S. P. and Fenn, J. B., 1978, "Experimental determination of the discharge coefficients for critical flow through an axisymmetric nozzle", Am. Inst. Aeronaut. Astronaut. J., vol.16, no.1,

pp.41-46.
2. Nakao, S., Yokoi, Y. and Takamoto, M., 1996, "Development of a calibration facility for small mass flow rates of gas and uncertainty of a sonic Venturi transfer standard", J. Flow Measmt Instrumentation, vol.7, pp.77-83.
3. Nakao, S., Irayama, T. and Takamoto, M., 2000, "Relations between the discharge coefficients of the sonic Venturi nozzle and kind of gases", J. Japan Soc. Mech. Engrs, Ser. B, vol.66, no.642, pp.438-444.
4. Johnson, R. C., 1965, "Real - gas effects in critical - flow - through nozzles and tabulated thermodynamic properties", NASA TN D-2565.
5. McCarty, R. D. and Weber, L. A., 1972, "Thermophysical properties of parahydrogen from the freezing liquid line to 5000R for pressures to 10,000 Psia", NBS TN 617.
6. McCarty, R. D.,Hord, J., and Roder,H.M, 1981, "Selected properties of hydrogen (engineering design data) ", NBS MN 168.
7. McCarty, R. D., 1975, "Hydrogen technological surveythermophysical properties", NASA SP 3089.
8. Nakao, S., 2005, "Development of critical nozzle flow meter for high pressure hydrogen gas flow measurements", In Proceedings of JSME, Fluid Dynamics Section, Kanazawa, Japan, G201.
9. Redlich, O. and Kwong, J.N.S, 1949, "On the Thermodynamics of Solutions. V (An Equation of State. Fugacities of Gaseous Solutions)", Chemical reviews, vol.44, pp.233-244.
10. Kishige, H., Teshima, K., Nishida, M., 1993, "Focusing of Shock Wave with Vibrational Relaxation Effect", Technology Reports of Kyushu University, vol.66, No. 2.
11. Launder, B. E. and Spalding , D. B., 1974, "Computer Methods in Applied Mechanics and Engineering", vol.3, pp.269-289.
12. Yee, H.C., 1989, "A class of high-resolution explicit and implicit shock capturing methods", NASA TM-89464.
13. ISO 9300, (1990).
14. Nakao, S., 2001, "A Study on the Conversion Factor of Sonic Venturi Nozzles", Proc. of NCSL International Workshop & Symposium.
15. Kim,H.D., Kim, J. H., Park,K. A., Setoguchi,T. and Matsuo, S., 2003, "Computational study of the gas flow through a critical nozzle", Proc. InstnMech. Engrs,Part C: J.Mechanical Engineering Science, Vol.217, No.10, pp.1179–1189.
16. Johnson, R. C., 1965, "Real-gas effects in critical - flow - through nozzles and tabulated thermodynamic properties", NASA TN D-2565.

6. NOMENCLATURE

Symbol	Meaning	Unit
A	Cross-section area	(m^2)
C_d	Discharge coefficient	(-)
C_v	Specific heat at constant volume	(J/kg·K)
D	Diameter of the critical nozzle throat	(m)
$\boldsymbol{E}$, $\boldsymbol{F}$	Inviscid flux vectors	(-)
E_t	Total energy per unit volume	(J/m^3)
$\boldsymbol{H_1}$	Source term for axsimmetry	(-)
$\boldsymbol{H_2}$	Source term for Turbulence	(-)
p	Pressure	(Pa)
p_b	Back pressure	(Pa)
R	Radius of the critical nozzle	(m)
$\boldsymbol{R}$, $\boldsymbol{S}$	Viscous flux vectors	(-)
Re	Reynolds number	(m)
T	Temperature	(K)
t	Time	(s)
$\boldsymbol{U}$	Conservative vector	(-)
u, v	Velocity components	(m/s)
v	Specific volume	(m^3/kg)
x, y	Cartesian coordinates	(m)
Z	Compressibility factor	(-)
Greeks		
γ	Ratio of specific heats	(-)
κ	Thermal conductivity	(W/m·K)
ρ	Density	(kg/m^3)
σ_t	Mass flow rate	(-)
τ	Shear stress	(Pa)
θ	Angle of attack	($^\circ$)
Subscripts		
0	Stagnation point	
c	Critical point	
t	Critical nozzle throat	
th	theory	

7.MAILING ADDRESS

Mamun Mohammad
Dept.of Mechanical Engineering, BUET
Dhaka-1000, Bangladesh